VIII International Conference on Fracture Mechanics of Concrete and Concrete Structures
FraMCoS-8
J.G.M. Van Mier, G. Ruiz, C. Andrade, R.C. Yu and X.X. Zhang (Eds)

NUMERICAL MODELLING OF TEXTILE REINFORCED CONCRETE

N. WILLIAMS PORTAL[*], K. LUNDGREN[†]

A.M. WALTER[††], J.O. FREDERIKSEN[††], L.N. THRANE[††]

[*, †] Chalmers University of Technology
Civil and Environmental Engineering, Structural Engineering
SE-412 96 Gothenburg, Sweden
e-mail: Natalie.Williams@chalmers.se, Karin.Lundgren@chalmers.se, www.chalmers.se

[††] Danish Technological Institute
Building Technology, Concrete
Gregersensvej 1, DK-2630 Taastrup, Denmark
e-mail: amkn@dti.dk, jlf@dti.dk, lnth@dti.dk, www.dti.dk

Key words: Non-linear finite element analysis, Textile Reinforced Concrete, Bond-slip behaviour

Abstract: The design and building construction industry is in need of a paradigm shift. One way of dealing with this need is by exploring the use of alternative building materials, such as Textile Reinforced Concrete (TRC). TRC encompasses a fine-grained concrete matrix reinforced by multi-axial textile fabrics, which replaces the traditionally used reinforcement methods. Investigations of new materials are necessary in order to quantify its expected structural performance and integrity.

The purpose of this study is to investigate the structural behaviour of a thin TRC slab under bending stress. Four-point bending tests were conducted on thin TRC specimens strengthened by carbon fibre textiles. One of the test configurations was modelled using non-linear finite element methods. The influence of varying the contact perimeter between the textile reinforcement mesh and the concrete matrix was also studied. The finite element software DIANA with the pre- and post-processor FX+ was used.

The numerical analysis primarily consisted of 2-D non-linear FE modelling of a thin TRC slab specimen. Cracking of the cement matrix was modelled with a smeared rotating crack model. The bond between the textile and the cement matrix was modelled using bond-slip, with input based on pull-out tests from literature. Simplified bi-linear stress-strain laws were assigned to the textile reinforcement. The main failure mode observed was in bending with the delamination of the textiles from the mortar or by the tensile failure of the textile.

1 INTRODUCTION

Sustainable development has become increasingly in demand within the building construction industry. New technological advances making use of non-traditional types or amounts of material and energy could be used to meet the demand for a sustainable industry [1]. An innovative material which is thought to have emerged from this idea is Textile Reinforced Concrete (TRC). TRC is a combination of fine-grained concrete and multi-axial textile fabrics, which has been fundamentally researched over the past decade [2]. This composite material has been shown to have the potential to be used to design slender, lightweight, modular and freeform

structures, while eliminating the risk of corrosion and providing high strength in compression and also in tension [2, 3]. It has also been proven to be a suitable solution for the strengthening of existing structures [4-7].

TRC is differentiated from ordinary steel reinforced concrete mainly by its complex heterogeneous structure. A textile reinforcement yarn consists of numerous filaments which inhibit the even penetration of the fine-grained concrete matrix between the filaments. The inner filaments, as a result, have less contact with the fine-grained concrete matrix depending on the size of the *fill-in zone* [8]. This phenomenon causes the damage localization process to be governed by the bond between the textile mesh and the fine-grained concrete matrix. Accordingly, the complex bond behaviour has become the driving force for developing numerical models in various scales: macro [9], meso [8-11], micro [12, 13] and multi [14-17]. However, there are difficulties to quantify the bond-slip relationship at different scales; and when incorporated, can become computationally demanding [9]. In this particular case, macro-scale modeling was chosen, to investigate whether that is a suitable level to model crack pattern and failure mode of a tested TRC specimen.

This paper presents the investigation of the structural behaviour of a thin TRC slab composed of a cement matrix and reinforced by a carbon fibre mesh under bending stress. This investigation is conducted by means of experimental testing and FE modelling. The experimental study reveals the influence of varying the mesh configuration and fibre density of the textiles within the structure. The development of a 2-D non-linear macro-scale model of this tested slab specimen is presented along with its verification. Furthermore, the influence of varying the contact perimeter existing between the textile reinforcement mesh and the concrete matrix is analysed and recommendations about further model development are presented.

2 EXPERIMENTAL TESTING

In this study, four-point bending tests of thin TRC slabs reinforced by carbon fibre textiles were carried out. The testing comprised of loading until complete failure which was defined by either delamination or failure of the textile itself. The measurements that were recorded during the testing included crack pattern, applied load and deformation.

2.1 Test details

The test specimens consisted of thin TRC slabs with dimensions of 800 mm in length, 200 mm in width, and 80 mm in height. The carbon textile mesh was placed at 7.5 mm from the bottom edge of the slab and casting was executed as per Figure 1.

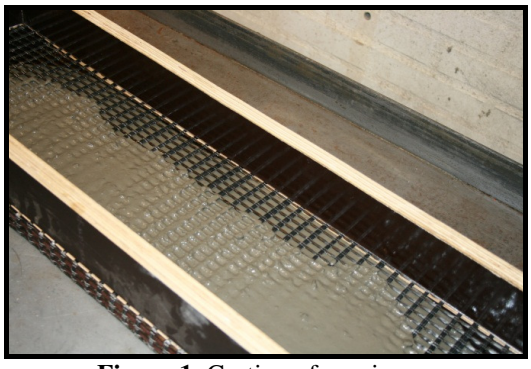

Figure 1: Casting of specimens

The specimens were stored in a sealed and dry environment of 30°C until reaching 28 days of maturity prior to undergoing four-point bending testing. Figure 2 and Figure 3 depict the described specimen geometry and the test setup.

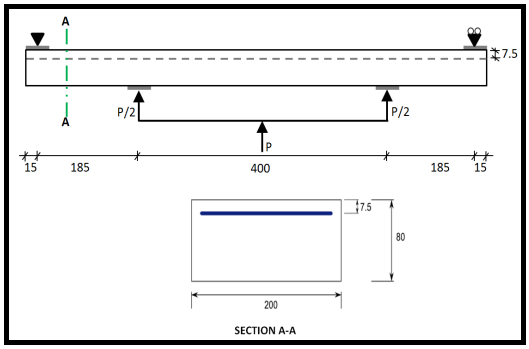

Figure 2: Specimen geometry four-point bending test setup.

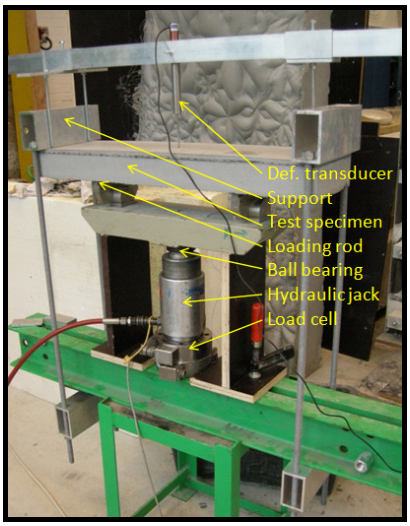

Figure 3: Setup of the four-point bending test.

In the test setup, the load was applied from beneath as shown in Figure 3. The test specimen was placed upside down compared to when it was casted. It was placed on a loading beam with two steel rods in between to apply two line loads. The support of the test specimen consisted of two alu-profiles. One of the steel rods and one of the alu-profiles could rotate in order to make sure that both line loads and line supports were uniformly distributed across the test specimen. The load was applied by a hydraulic jack placed on a load cell. A deformation transducer was mounted on an alu-profile on top of the test specimen in order to measure mid-span deflection relative to the supports. During testing, the deformation and load were measured and stored every second using a data logger.

2.2 Materials

The textile reinforcement selected for this experimental study was composed of weaved carbon fibres. Carbon fibres are defined as heavy-tow-yarns, which signifies that they have a higher yarn cross-section; as such, a higher load-bearing capacity of the structure is expected [18]. These textile meshes were purchased from the European Institute for Advanced Textile Technology and Textile Machinery (TUDATEX) which is part of the Dresden University of Technology AG Company (TUDAG). As illustrated in Figure 4, three different carbon textile meshes categorized as, *Fine*, *Medium* and *Coarse*, were included in the experimental study.

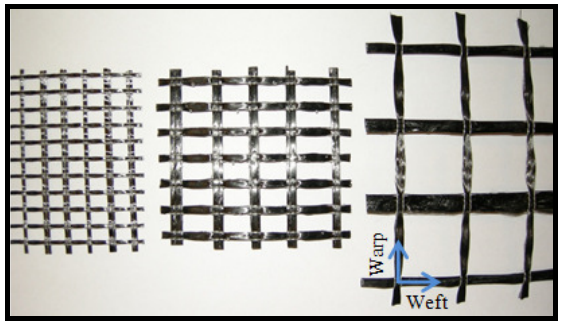

Figure 4: Carbon fibre textile meshes included in the experimental study.

The carbon fibre properties vary according to that provided in Table 1. It should be noted that the linear density is measured in *tex*, which is equivalent to 1 g of fibre per 1000 m.

Table 1: Carbon fibre properties

Textile Mesh	No. filaments [k= x·10^3]	Linear density [tex]	Weft (90°) [mm]	Warp (0°) [mm]
Fine	12k	800	11	7
Medium	50k	3500	18	11
Coarse	50k	3500	30	30

Furthermore, small cross-sections of each textile mesh were impregnated with fluorescent epoxy in order to enable microscopy-images of the yarn structure. The magnified cross-section of the *Medium* textile mesh, for example, is depicted below in Figure 5.

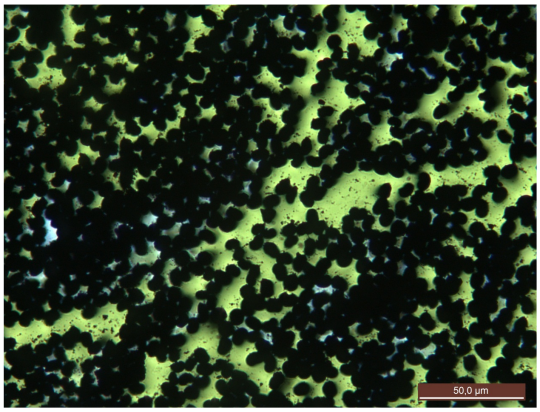

Figure 5: Magnification of one thin section of the epoxy impregnated carbon fibre yarn (Scale: 50.0 µm).

In Figure 5, the following observations can be drawn: filaments are easily detected in *black; fluorescen*t *yellow* indicates epoxy penetrated between the filaments; and lastly, *white* shows zones which are not in contact with epoxy.

It was necessary to obtain data such as mechanical properties from literature corresponding to a similar carbon textile to develop the FE model. Mechanical properties corresponding to a carbon textile having the same weft and warp dimensions as specified for the *Medium* alternative are provided in Table 2.

Table 2: Mechanical properties for carbon textile [18]

Textile Material	Linear density [tex]	Tensile Strength [N/mm^2]	Failure strain [‰]	Young's Modulus [N/mm^2]
Carbon	3300	1200	12	100 000

Due to a lack of available material data corresponding to the tested textile mesh alternatives, the developed model was limited to the simulation of the *Medium* alternative. The thin TRC slabs also consisted of a fine-grained concrete matrix. The mix composition of the selected matrix amounts to a water-cement ratio of 0.42 (w/ceq=0.33) and is summarized in Table 3.

Table 3: Mix composition of the fine-grained concrete matrix

Material	Weight [kg]	Density [kg/m^3]	Abs/ moist	m^3/m^3
Low-alkali cement	406	3200		0.127
Fly ash	121	2300		0.053
Mircrosilica	22	2200	0	0.010
0/4 sand	1400	2640	0.2	0.530
Glenium SKY 532-SU	7.6	1100	68	0.007
Amex SB 22	3	1010	98.2	0.003
Water	170.56	1000		0.171
Air				0.100
Total	*2130.16*			*1.000*

Other properties related to the fine-grained concrete were not measured in this study. The mechanical properties of a similar fine-grained concrete mixture were therefore used as input in the FE model. The mechanical properties for the concrete were taken from [18] such that the average compressive strength of a cube specimen was taken as 45.5 N/mm^2 and the average bending strength as 5.7 N/mm^2. It should be noted that the compressive strength was corrected as per EC2 for a cylindrical sample which gives 38 N/mm^2 and the tensile strength was assumed to be equivalent to the bending strength.

The E-modulus included in the model was taken as 26 150 N/mm^2 [18], which corresponds to a similar concrete mixture used in the experimental study. It is important to highlight that the E-modulus of the concrete is in fact the governing stiffness at the beginning of the loading of an un-cracked TRC specimen (State I) [3]. As such, it is considerably important to define this property appropriately in order to yield representative simulation results.

2.3 Test results

The results from the four-point bending test for all three carbon textile mesh alternatives are presented below in Figure 6 and summarized in Table 4.

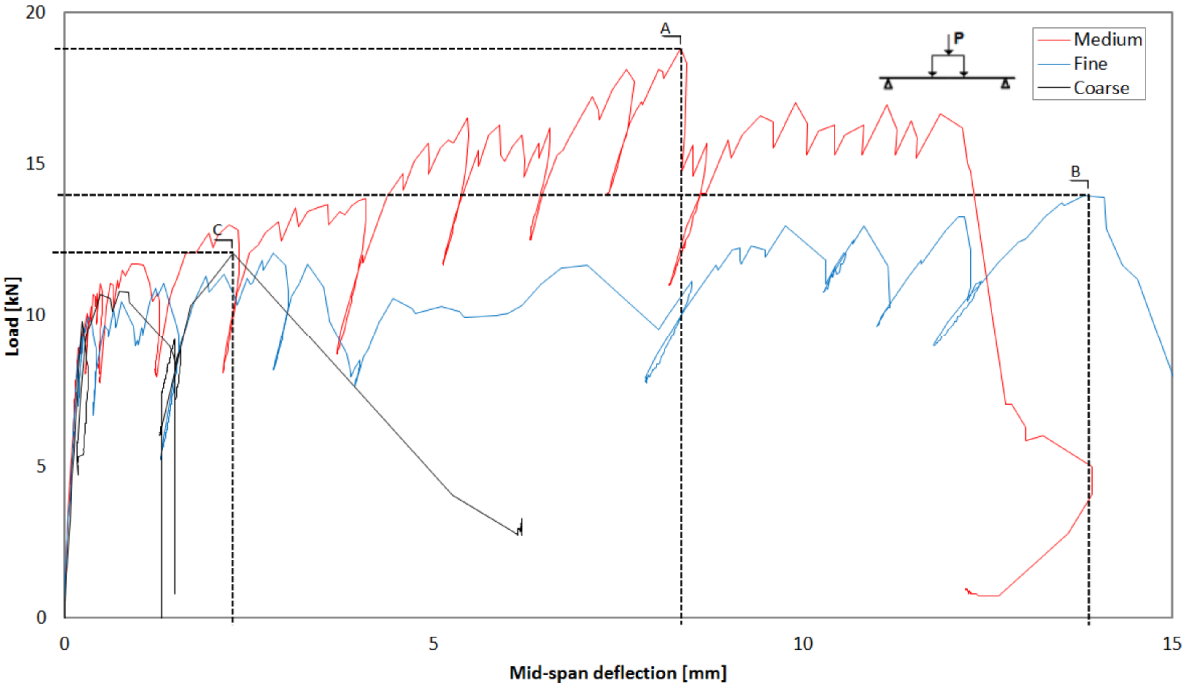

Figure 6: Experimental results for all specimens – Load [kN] versus mid-span deflection [mm].

Table 4: Summary of experimental results

Textile	Initial Cracking Load [kN]	Max Load [kN]	Total deflection [mm]	Total number cracks
Medium (A)	11	18	8	11
Fine (B)	10	13	14	6
Coarse (C)	10	12	2	2

It is observed from Table 4 that all three alternatives began cracking at approximately 10 kN. Thereafter, multiple through-going cracks appeared in all three specimens until failure was reached. Delamination of the textile caused the failure of *Medium* and *Fine* specimens, while textile failure occurred in the *Coarse* specimen. The *Medium* mesh withheld the highest load of 18 kN and the *Fine* mesh had the highest ductility of 14 mm. The higher load bearing capacity of the *Medium* mesh was expected due to the fact that it has the largest cross-sectional area. Furthermore, it should be noted that with a longer anchorage length, the bond between the textile mesh and the fine-grained concrete matrix could potentially be improved for all textile types.

3 FE MODEL DEVELOPMENT

A 2-D non-linear macro-scale FE model of a thin TRC slab was developed to further investigate its structural behaviour under bending stress. The model was developed using the finite element analysis software DIANA with pre- and post-processor FX+ [19]. The verification of the FE model was accomplished by means of the experimental results obtained from the four-point bending testing.

3.1 Loading and boundary conditions

The symmetry of the mounting and loading of the tested TRC specimens allows for half of the span and loading to be considered in the model as depicted in Figure 7. The thin slabs were loaded until failure by half of the applied load, denoted as *P/2*. The self-weight of the slabs were not included in the analyses; since its contribution to the bending moment at mid-span is less than 2e-4%, its effect on the results is negligible.

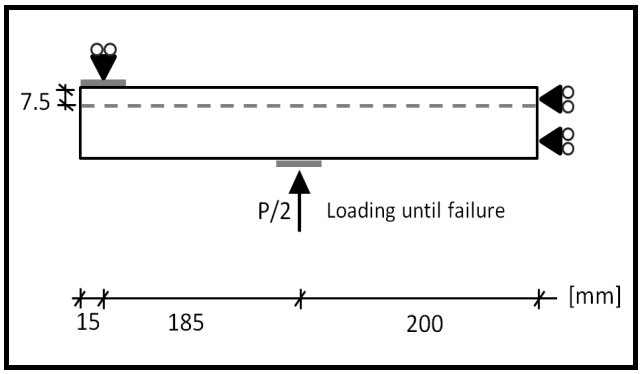

Figure 7: Half of the thin slab with defined loading and constraints.

The loading until failure was applied to the slab by means of displacement control, such that an imposed displacement was applied at the location of loading.

3.2 Element types

The model developed in DIANA included 2-D plane stress elements for concrete *(Q8MEM)*, 1-D truss-bar elements for textile reinforcement *(L2TRU)*, along with 2-D line-interface elements with bond-slip *(L8IF)*. The 2-D line-interface elements created an interface between two lines in a two-dimensional configuration. In this case, the interface elements were aligned with the truss-bar elements and accordingly they shared the same nodes. The interface elements were also connected to the 2-D plane stress elements by linking their closest adjacent nodes. This connectivity is depicted in Figure 8.

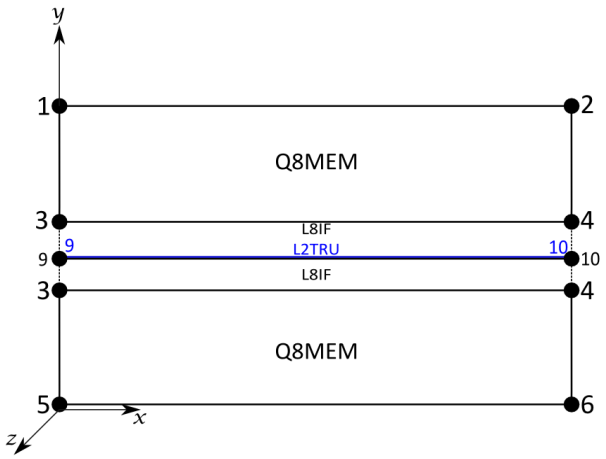

Figure 8: Connectivity of 2-D plane stress elements (Q8MEM) and 1-D truss-bar elements (L2TRU) with 2-D line-interface elements (L8IF).

A stiff plate at the prescribed support locations was modelled by including a stiff 2-D class I-beam element located at the middle node of the support along with eccentric tying of the surrounding nodes. Essentially, the nodes found within the actual support geometry are slaved to the eccentric tying node (middle node). The purpose of including these elements is to prevent localized failure. An overview of the model developed in FX+ is shown in Figure 9 and the corresponding element and model definitions are described in Table 5.

Table 5: Precribed elements in the model

Affected area	Element type	No. nodes	No. elements
Concrete	2D quadrilateral plane stress *(Q8MEM)*	4	1806
Textile	1D truss bar *(L2TRU)*	2	86
Interface	2D line-interface *(L8IF)*	4	86
Supports (Stiff beams)	2D class I-beam *(L6BEN)*	2	2

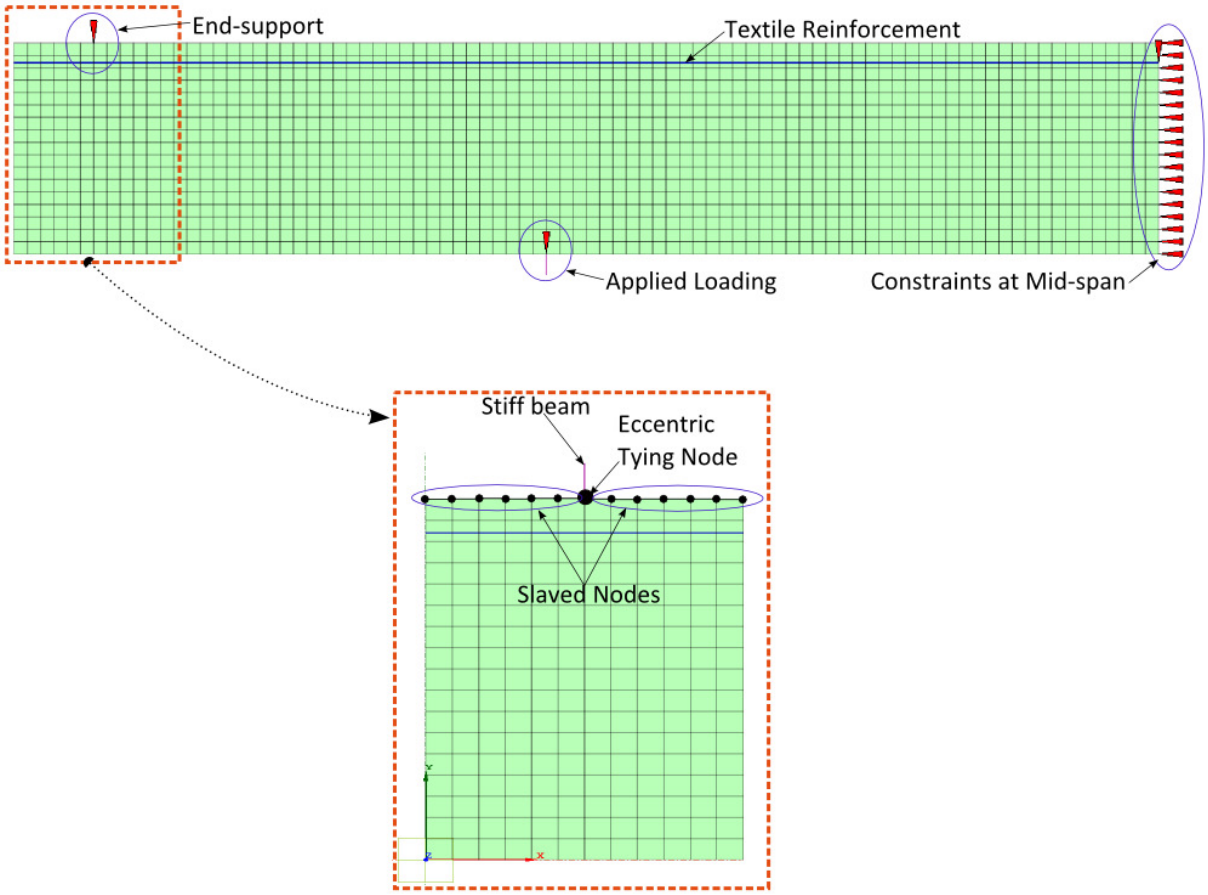

Figure 9: Overview of the developed model.

3.3 Material characterization

A non-linear macro-scale model is used to idealize smeared and homogenized material components and properties for the thin TRC slab. The simplification of the developed model is formulated based on the Aveston-Cooper-Kelly (ACK) analytical model. This analytical approach, idealized in Figure 10, describes the behaviour of multi-cracked composites under tensile loading while treating the textile reinforcement as a monolithic bar [20]. Accordingly, the model incorporates one rigid bond at the interface between the cement matrix and the monolithic textile reinforcement (or grouping of yarns). This simplification neglects the potential relative displacement between the internal and external filaments of a yarn, but is still found to be adequately accurate according to [9].

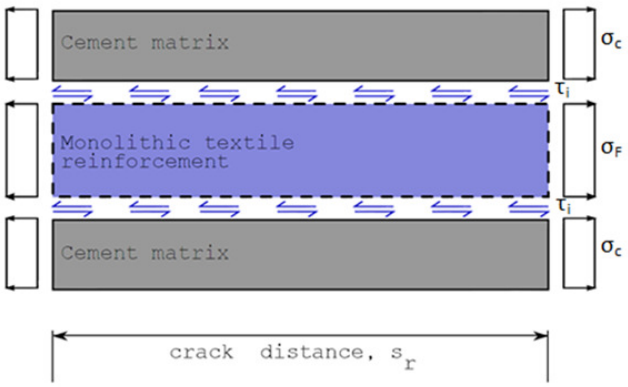

Figure 10: Idealization of the textile reinforced concrete model (based on [9, 14]).

The bond-slip relationship between the textile and the fine-grained concrete matrix was incorporated in the model to simulate the bond. This data is typically obtained by means of pull-out tests, which were not included in the scope of the experimental study. A bond-slip relationship for a similar combination of

TRC obtained from [18] was thus included in the model. The bond-slip relationship is defined according to a multi-linear model in DIANA and is depicted below in Figure 11.

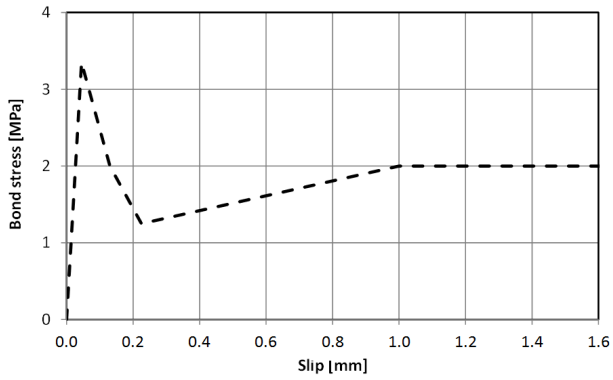

Figure 11: Bond-slip relationship for carbon textile reinforcement [18].

In the developed model, the textile reinforcement mesh was simplified by grouping each yarn into a monolithic textile reinforcement. Accordingly, the cross-section of one fibre yarn was considered and multiplied according to a given number of fibre rovings satisfying a given unidirectional mesh spacing along the total width of the specimen, as shown in Figure 12.

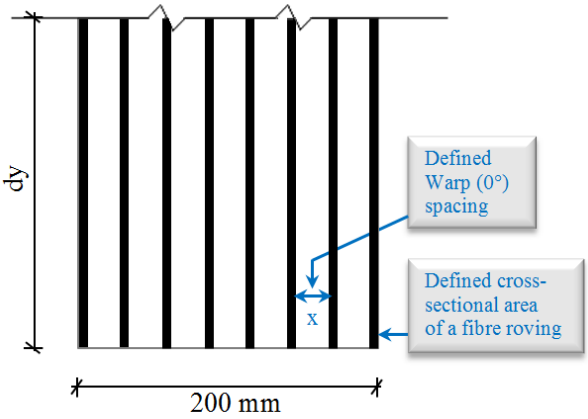

Figure 12: Grouping of textile reinforcement geometry.

It should be noted that since the thin-slab is loaded in bending, the mesh could be simplified assuming unidirectional fibres. The orientation in which the *Medium* textile mesh was placed is presumed to have a yarn spacing distance of 11 mm along the width of the slab. In order to obtain monolithic textile reinforcement, the cross-section of a fibre yarn was calculated according to Equation 1 [4]:

$$A_{f,Roving} = \frac{linear\ density\ [tex(\frac{g}{1000m})]}{density\ [\frac{kg}{m^3}]} \quad (1)$$

Moreover, a total strain based crack model with rotating crack was defined for the fine-grained concrete. In DIANA, this type of model requires the specification of tension softening and compressive behaviours. Accordingly, a non-linear Hordijk tension softening model and Thorenfeldt compression curve were included. The Thorenfeldt curve was included in order to yield more realistic concrete compression failure by incorporating a softening behaviour of concrete in compression. This model, however, is based on 300 mm long cylinder specimens, and as such, should be corrected after the peak when applied to smaller element sizes according to [21]. Concerning the developed FE model, an adjustment of the Thorenfeldt curve was found to be necessary to compensate for the small element size (4.625 mm). In tension, a crack band width equal to the element size was chosen, thus assuming that the cracks would localize in single element rows. This will be further discussed in Section 4.2.

The stress-strain law assigned to the textile reinforcement is shown in Figure 13.

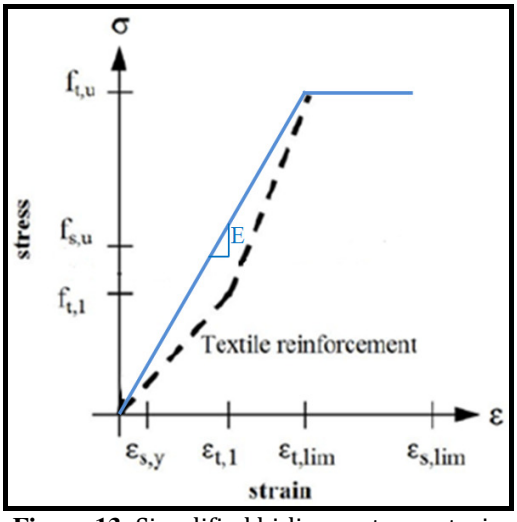

Figure 13: Simplified bi-linear stress-strain relationship for carbon-textile reinforcement [18].

An ideally-plastic simplification of a bi-linear relationship, shown by the solid line in Figure 13, was assumed in the model.

4 NUMERICAL SIMULATIONS

The numerical simulations results obtained from the developed 2-D non-linear macro-scale model are presented and compared with the experimental results. The contact perimeter was a parameter which was primarily varied in the simulations, as it was found to have a significant impact on the overall load-bearing behaviour of the thin TRC specimen. In the analysis, this parameter corresponds to the thickness of the bond interface. Moreover, the load versus mid-span displacement curves are compared, along with the observed crack patterns.

4.1 Bond interface

In the developed macroscopic model, the contact perimeter of the bond interface was found to be an important parameter. In order to be able to extract a bond-slip relationship from pull-out tests, the total contact perimeter between the yarns and the concrete matrix should be estimated or measured. However, this input data was not available, and, as such, its sensitivity was evaluated in this study.

As illustrated below in Figure 14, the actual contact between the yarns, as well as the penetration of the concrete matrix between the yarns could influence the bond-slip relationship. It is rather difficult to quantify these phenomena, particularly in macroscopic scale; therefore, the yarns were assumed to have a rectangular contact perimeter.

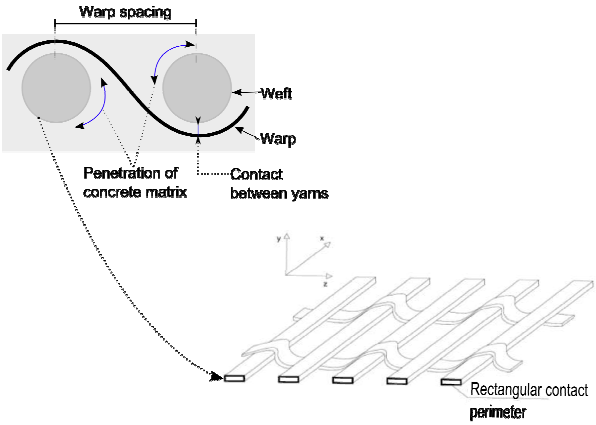

Figure 14: Idealization of contact perimeter between yarns and concrete matrix.

The ratio between the width and thickness of the rectangular perimeter was varied in order to observe the sensitivity of the contact perimeter in the modeling. The outcome of perimeter variation is presented and further discussed in Section 4.2.

4.2 Result Comparison

A comparison between the simulation results and the experimental results corresponding to the *Medium* textile mesh is illustrated in Figure 15 and summarized in Table 6.

Table 6: Summary of simulation results

Perimeter ratio (width:thick)	Contact perimeter [m]	Max Load [kN]	Total deflection [mm]
Medium		*18*	*8*
1:2	0.10	17.56	7.61
1:5	0.13	17.58	7.46
1:25	0.25	17.76	6.76
1:100	0.49	17.33	10.37
1:5000	3.5	17.50	16.16
1:20000	6.9	17.50	12.73

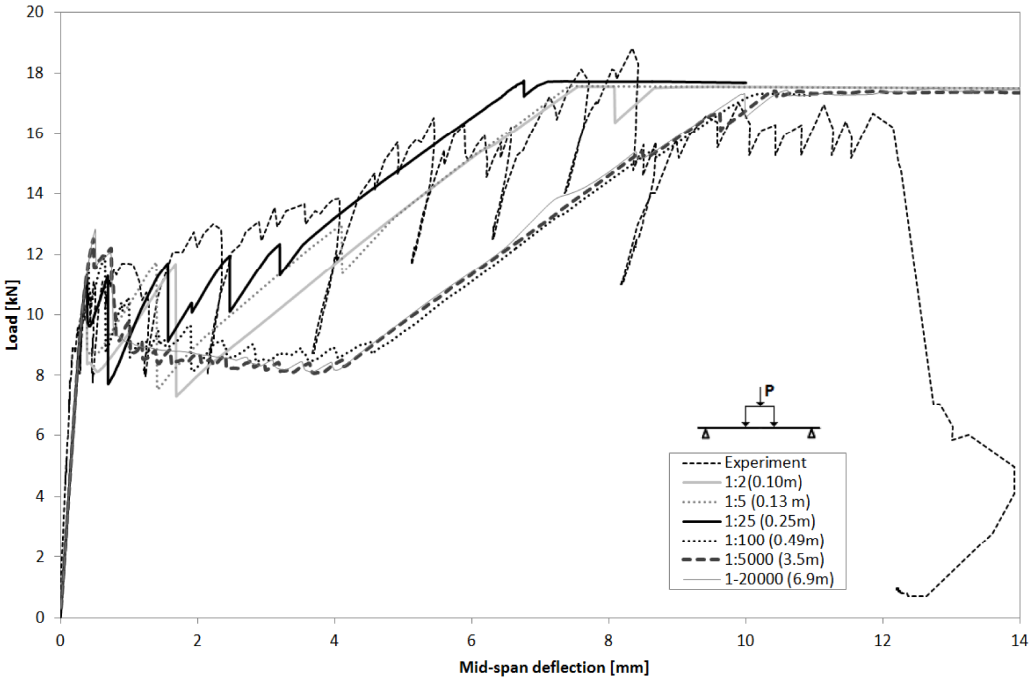

Figure 15: Load versus mid-span deflection: Comparison between simulation and experimental results.

As mentioned before, delamination of the textile caused the failure in the test. However, in all analyses, failure was primarily caused by fracture of the textile. In Figure 15, this occurs when the load-deflection curve reaches a constant slope; this behaviour is also consistent with the chosen ideally-plastic behavior of the textile reinforcement. It should be noted, that since the textile in reality shows a brittle fracture, the results should be interpreted so that total failure would occur in the analyses when the plateau is reached. Along with this failure mode, concrete crushing occurred at the lowest extremities of the cracks in the analyses. Thus, the 2D analyses could not correctly describe the delamination failure occurring in the test.

The initial stiffness described by each analysis correlated relatively well with that of the test, as shown in Figure 15. All analyses reached approximately the same maximum load of 18 kN as in the test, but revealed differences in ductility. The mid-span deflection at failure, evaluated as when the plateau was reached, was either slightly less or significantly greater than that of the test, as summarized in Table 6.

The solution corresponding to a ratio of *1:25* is observed to best correlate with the experimental load deflection in Figure 15, and crack pattern results in Figure 16. In this analysis, and also in the analyses with smaller contact perimeter, the assumption about cracks localizing in single element rows was correct. As can be expected, the contact perimeter affected both the crack pattern and the stiffness in the cracked region in this study. The smaller the contact perimeter, the larger crack distance and thus fewer cracks were observed. For large contact perimeters, the bond behaviour was observed to approach full interaction. The failure in these analyses took place in a crack that localized in a single element row, however in the rest of the tensile region, a diffuse crack pattern with almost all elements cracked were noticed, as per Figure 16. Thus, the assumption that cracks will localize in single element rows can then be questioned; in parts of the model it would be more proper to use a crack band width approximately equal to the crack spacing in reality.

The ratio between the width and thickness of the rectangular perimeter of *1:25* which agreed best with the experimental results corresponds to a width of 6.8 mm of each yarn. This width is approximately 62 % of the center distance between the yarns (11 mm).

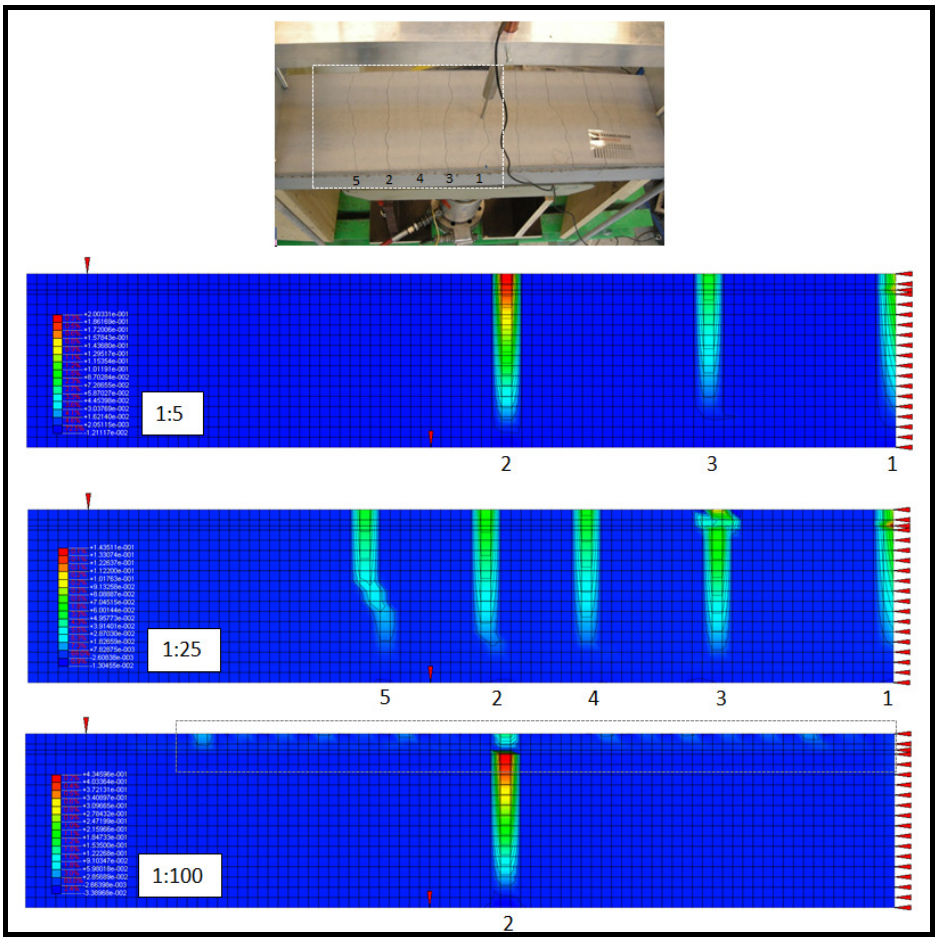

Figure 16: Crack pattern results compared to simulation results corresponding to *1:5*, *1:25* and *1:100*.

5 CONCLUSIONS AND OUTLOOK

The investigation of the thin TRC slab under bending stress revealed that the *Medium* specimen had the highest load bearing capacity (18 kN), while the *Fine* specimen had the highest ductility (14 mm). Delamination of the textile caused the failure of *Medium* and *Fine* specimens, while textile failure occurred in the *Coarse* specimen. With an increase in the anchorage length, the textile bond is expected to be improved. The development of a 2-D non-linear macro-scale model of the *Medium* specimen in DIANA FX+ was presented. The influence of varying the contact perimeter of the bond interface was analysed and the results were compared to the experimental results. In all analyses, fracture of the textile caused the failure, while as mentioned the failure mode in the test was delamination. The analysis assuming a ratio of *1:25* between the width and thickness of the rectangular perimeter, corresponding to a contact perimeter of 0.25 m, was found to best correlate with the load-deflection curve and the crack pattern in the test. The analyses also showed that as the contact perimeter increased, full interaction between the textile mesh and the concrete matrix was approached.

The FE model could be further improved by including the bi-linear stress-strain relationship for the textile reinforcement. Furthermore, possible ways to model the delamination could be examined. One way to include this in a 2D model could be to weaken the concrete elements surrounding the textile. As such, this simulates that the concrete below and above the textile is only in contact in between the textile yarns, and that it might not completely penetrate the mesh either. Another possibility is to turn to 3D modelling. Finally, it would have been beneficial to test the mechanical properties, such as the strength of the textile and the concrete and the bond between them,

instead of using data from literature as implemented here. Future experimental tests are planned to include these details.

6 ACKNOWLEDGEMENT

The presented research was funded by the European Community's Seventh Framework Programme under grant agreement NMP2-LA-2009-228663 (TailorCrete) and FORMAS (Homes for Tomorrow). More information about the research projects, TailorCrete and Homes for Tomorrow, can be found at www.tailorcrete.com and www.homesfor tomorrow.se, respectively.

REFERENCES

[1] Vanegas, J.A., DuBose, J. R. and Pearce, A. R., 1996. Sustainable Technologies for the Building Construction Industry. in *Proceedings of the Symposium on Design for the Global Environment*, Atlanta, USA, November 2-4, 1996.

[2] Orlowsky, J. and Raupach, M., 2011. *Textile reinforced concrete - from research to application.* Cement Wapno Beton, **16**(6): p. 323-331.

[3] Brameshuber, W., ed. Textile Reinforced Concrete, State-of-the-Art Report of RILEM Technical Committee 201-TRC. RILEM Report 36. 2006, RILEM Publication: Bagneux, France

[4] Ortlepp, R., Weiland, S., and Curbach, M., 2009. Rehabilitation and strengthening of a hypar concrete shell by textile reinforced concrete. in *Proceedings of International Conference on Concrete Construction*, London, Sept 9-10, 2008. pp.357-363.

[5] Ortlepp, R., Schladitz, F., and Curbach, M., 2011. *TRC strengthened RC columns.* Textilbetonverstärkte Stahlbetonstützen, **106**(9): p. 640-648.

[6] Schladitz, F., Lorenz, E., and Curbach, M., 2011. *Bending capacity of reinforced concrete slabs strengthened with textile reinforced concrete.* Biegetragfähigkeit von textilbetonverstärkten Stahlbetonplatten, **106**(6): p. 377-384.

[7] Bruckner, A., Ortlepp, R., and Curbach, M., 2006. *Textile reinforced concrete for strengthening in bending and shear.* Materials and Structures, **39**(8): p. 741-748.

[8] Hartig, J., Häußler-Combe, U., and Schicktanz, K., 2008. *Influence of bond properties on the tensile behaviour of Textile Reinforced Concrete.* Cement and Concrete Composites, **30**(10): p. 898-906.

[9] Holler, S., Butenweg, C., Noh, S.Y., and Meskouris, K., 2004. *Computational model of textile-reinforced concrete structures.* Computers & Structures, **82**(23-26): p. 1971-1979.

[10] Hegger, J., Will, N., Bruckermann, O., and Voss, S., 2006. *Load–bearing behaviour and simulation of textile reinforced concrete.* Materials and Structures, **39**(8): p. 765-776.

[11] Häußler-Combe, U. and Hartig, J., 2007. *Bond and failure mechanisms of textile reinforced concrete (TRC) under uniaxial tensile loading.* Cement and Concrete Composites, **29**(4): p. 279-289.

[12] Chudoba, R., Vořechovský, M., and Konrad, M., 2006. *Stochastic modeling of multi-filament yarns. I. Random properties within the cross-section and size effect.* International Journal of Solids and Structures, **43**(3–4): p. 413-434.

[13] Vořechovský, M. and Chudoba, R., 2006. *Stochastic modeling of multi-filament yarns: II. Random properties over the length and size effect.* International Journal of Solids and Structures, **43**(3-4): p. 435-458.

[14] Peiffer, F., 2008. Framework for adaptive simulations applied to textile reinforced concrete. PhD thesis, RWTH Aachen University

[15] Lepenies, I.G., 2007. *Zur hierarchischen und simultanen Multi-Skalen-Analyse von Textilbeton*. Ph.D. thesis, Technical University of Dresden.

[16] Ernst, G., Vogler, M., Hühne, C., and Rolfes, R., 2010. *Multiscale progressive failure analysis of textile composites.* Composites Science and Technology, **70**(1): p. 61-72.

[17] Graf, W., Hoffmann, A., Möller, B., Sickert, J.-U., et al., 2007. *Analysis of textile-reinforced concrete structures under consideration of non-traditional uncertainty models.* Engineering Structures, **29**(12): p. 3420-3431.

[18] Schladitz, F., Frenzel, M., Ehlig, D., and Curbach, M., 2012. *Bending load capacity of reinforced concrete slabs strengthened with textile reinforced concrete.* Engineering Structures, **40**(0): p. 317-326.

[19] TNO DIANA. Finite Element Analysis User's Manual - Release 9.4.4, TNO, 2011.

[20] Aveston, J., Cooper, G. A., and Kelly, A. Single and Multiple Fracture. in *Proceedings of the Conference on the Properties of Fibre Composites*, 1971, National Physical Laboratory,IPC Science & Technology Press, Guildford, UK. pp.15-26.

[21] Zandi Hanjari, K., 2008. *Load-carrying capacity of damaged concrete structures*. Lic, in *Civil and Environmental Engineering*. Chalmers University of Technology: Gothenburg, SE.